# AN ELASTIC ISOTROPIC, PLASTIC ORTHOTROPIC CONSTITUTIVE MODEL BASED ON DEVIATOR TRANSFORMATIONS

## K. HEIDUSCHKE

Alusuisse Technology & Management Ltd., Technology Center,
8212-Neuhausen am Rheinfall, Switzerland

**Abstract**—A strain space description of an elastic isotropic, plastic orthotropic constitutive model is presented, which introduces the plastic orthotropy into the classical $J_2$-theory by a transformation of the elastic strain deviator. The constitutive model is physically similar to Hill's model, to which it is compared analytically. It is implemented in a sheet metal forming finite element program, of which simulation results on earing effects are shown. The orthotropic plasticity algorithm resulting from the deviator transformation is an explicit constitutive algorithm and, therefore, numerically efficient. © 1997 Elsevier Science Ltd.

## 1. INTRODUCTION

The orthotropic plasticity model introduced by Hill (1948) is based on second order yield (or loading) functions, which restricts its generality to some extent. Nevertheless, for the numerical treatment of orthotropic plasticity it is most widely used in computer simulation programs. Most of these orthotropy implementations use implicit constitutive algorithms in which tensor quantities are iterated. Especially for vectorization, where a block of, say, $N$ finite element integration points is treated at one fell swoop, the computational performance of implicit constitutive algorithms is usually worse than the performance of comparable explicit algorithms, since in implicit algorithms a whole block of $N$ integration points must wait until the iterations of all members have converged. In explicit algorithms, on the other hand, the number of operations is the same for all members, there are no waiting block members. Therefore, the computation vector performance of explicit constitutive algorithms is, in general, better than the performance of implicit algorithms.

In the present study we propose a model of orthotropic plasticity, which is similar to Hill's model, but which is based on orthotropic tensor transformations of the elastic strain. By using mappings of orthotropic yield surfaces to von Mises-like yield surfaces, the well-known and numerically effective constitutive algorithm for isotropy, namely the radial return method of Krieg and Krieg (1977), can be expanded to orthotropic plasticity without losing numerical efficiency.

The constitutive description is performed in the strain space, which is based on the kinematic variables (total) strain $\varepsilon$ and plastic strain $\varepsilon^p$. This is an adequate and natural description for displacement-based or kinematic finite elements, which are most widely used throughout nonlinear analysis. According to Casey and Naghdi (1983) the strain space and stress space descriptions are not equivalent. Following Moss (1984) we recall the computational significance of the strain space formulation, and following Naghdi (1990), page 337, we recall its primacy.

We consider isotropic, linear stress–strain relations, second-order yield functions with "associated" flow rules in the transformed strain spaces and isotropic hardening laws, similar to the models of Hill (1948) and (1979). We introduce the plastic orthotropy into the constitutive model by transformations of elastic strain deviators and discuss the differences between the model presented and Hill's model. We focus on the constitutive equations, for which we need physically meaningful definitions of strain traces and strain deviators. These definitions are well-established for the infinitesimal deformation theory.

Within the framework of finite deformation theory they are given in Heiduschke (1995), (1996) and the references cited therein.

The motivation for the developments presented is to produce an explicit algorithm with high vector performance for the implementation in finite element programs. A sheet metal forming constitutive algorithm, whose isotropic version has been presented by Heiduschke *et al.* (1991), is implemented in the finite element simulation program AutoForm, for which simulations concerning the earing effect of deep drawn circular sheet metal are shown.

## 2. DEVIATOR TRANSFORMATION

We call the abbreviation

$$\varepsilon^{e} = \varepsilon - \varepsilon^{P} \tag{1}$$

elastic strain, which is well accepted for infinitesimal deformations. Within the concept of the finite deformation theory we emphasise that (1) is not defined by means of any so-called intermediate stress free configuration. The abbreviation $\varepsilon^{e}$ is just the difference of the (total logarithmic) strain $\varepsilon$ and the (logarithmic) plastic strain $\varepsilon^{P}$, which are tensors with respect to the reference configuration $\kappa_0$.

We introduce a tensor transformation on the elastic strain

$$\hat{\varepsilon}^{e} = \omega\varepsilon^{e} \quad \text{and} \quad \hat{\varepsilon}^{e}_{ij} = \omega_{ijkl}\varepsilon^{e}_{kl}, \tag{2}$$

respectively written in symbolic and component notation, where $\hat{\varepsilon}^{e}$ denotes the transformed elastic strain deviator, $\omega$ the orthotropic fourth-order transformation tensor and where the summation convention is applied on repeated indices, i.e. on $k$ and $l$ in eqn (2b). In a coordinate system pointing in principal material directions the non-zero components of $\omega$ are

$$\omega_{1111} = L + M, \quad \omega_{2222} = M + N, \quad \omega_{3333} = N + L,$$

$$\omega_{1122} = \omega_{2211} = -M, \quad \omega_{2233} = \omega_{3322} = -N, \quad \omega_{3311} = \omega_{1133} = -L,$$

$$\omega_{1212} = \omega_{1221} = \omega_{2112} = \omega_{2121} = \tfrac{3}{2}O,$$

$$\omega_{2323} = \omega_{2332} = \omega_{3223} = \omega_{3232} = \tfrac{3}{2}P, \quad \omega_{3131} = \omega_{3113} = \omega_{1331} = \omega_{1313} = \tfrac{3}{2}Q. \tag{3}$$

The orthotropy coefficients $L$, $M$, $N$, $O$, $P$, $Q$ are similar† to Hill (1948, 1979 and 1987). The components of the fourth-order tensor $\omega$ fulfil

$$\omega_{iikl} = 0 \quad (\text{sum on } i) \tag{4}$$

and the symmetries

$$\omega_{ijkl} = \omega_{ijlk} = \omega_{jikl} = \omega_{klij}. \tag{5}$$

The tensor transformation (2) results in a deviator, since eqn (4) holds and $\hat{\varepsilon}^{e}_{kk} = 0$. It is therefore called a deviator transformation. The transformation inverse to (2) is

$$\varepsilon'^{e} = \rho\hat{\varepsilon}^{e}, \quad \varepsilon'^{e}_{ij} = \rho_{ijkl}\hat{\varepsilon}^{e}_{kl}, \tag{6}$$

where

† See Section 5 for the comparison with Hill's model.

$$\boldsymbol{\varepsilon}'^{\mathrm{e}} = \boldsymbol{\varepsilon}^{\mathrm{e}} - \tfrac{1}{3}\varepsilon_{kk}\mathbf{1}$$

denotes the elastic strain deviator and $\mathbf{1}$ the second-order unit tensor, which components are given by Kronecker's $\delta_{ij}$. The deviatoric inverse to $\omega$, denoted by $[\cdot]^{-1'}$, is the fourth-order tensor

$$\boldsymbol{\rho} = [\omega]^{-1'} \tag{7}$$

which obeys

$$\boldsymbol{\rho}\omega = \omega\boldsymbol{\rho} = \mathbf{1}', \quad \rho_{ijop}\omega_{opkl} = \omega_{ijop}\rho_{opkl} = \mathbf{1}'_{ijkl}, \tag{8}$$

where $\mathbf{1}'$ is the deviatoric fourth-order unit tensor with the components

$$\mathbf{1}'_{ijkl} = \tfrac{1}{2}(\delta_{ik}\delta_{jl} + \delta_{il}\delta_{jk}) - \tfrac{1}{3}\delta_{ij}\delta_{kl}.$$

The tensors $\mathbf{1}'$ and $\boldsymbol{\rho}$ obey the condition (4) and the symmetries (5) (Hill, 1987). In a coordinate system pointing in principal material directions the non-zero components of $\boldsymbol{\rho}$ are

$$\rho_{1111} = \frac{1}{9}\frac{L+M+4N}{LM+MN+NL}, \quad \rho_{2222} = \frac{1}{9}\frac{M+N+4L}{LM+MN+NL}, \quad \rho_{3333} = \frac{1}{9}\frac{N+L+4M}{LM+MN+NL},$$

$$\rho_{1122} = \rho_{2211} = \frac{1}{9}\frac{M-2(N+L)}{LM+MN+NL}, \quad \rho_{2233} = \rho_{3322} = \frac{1}{9}\frac{N-2(L+M)}{LM+MN+NL},$$

$$\rho_{3311} = \rho_{1133} = \frac{1}{9}\frac{L-2(M+N)}{LM+MN+NL}, \quad \rho_{1212} = \rho_{1221} = \rho_{2112} = \rho_{2121} = \frac{1}{6O},$$

$$\rho_{2323} = \rho_{2332} = \rho_{3223} = \rho_{3232} = \frac{1}{6P}, \quad \rho_{3131} = \rho_{3113} = \rho_{1331} = \rho_{1313} = \frac{1}{6Q}.$$

In the case of isotropy the condition

$$L = M = N = O = P = Q = \tfrac{1}{3} \tag{9}$$

should hold so that

$$\omega = \rho = \mathbf{1}'.$$

The condition (9) is later used to determine a free constant. For isotropy as specified by eqn (9) the transformation (2) simply maps the elastic strain $\boldsymbol{\varepsilon}^{\mathrm{e}}$ into its deviator $\boldsymbol{\varepsilon}'^{\mathrm{e}}$ and the corresponding reverse transformation (6) is a unit transformation, which leaves deviators unchanged.

## 3. CONSTITUTIVE MODEL

Besides the original (total logarithmic) strain

$$\boldsymbol{\varepsilon} = \boldsymbol{\varepsilon}^{\mathrm{e}} + \boldsymbol{\varepsilon}^{\mathrm{p}},$$

which has already been discussed with the abbreviation (1), we define the transformed total strain deviator by

$$\tilde{\boldsymbol{\varepsilon}} = \hat{\boldsymbol{\varepsilon}}^{\mathrm{e}} + \boldsymbol{\varepsilon}^{\mathrm{p}} \tag{10}$$
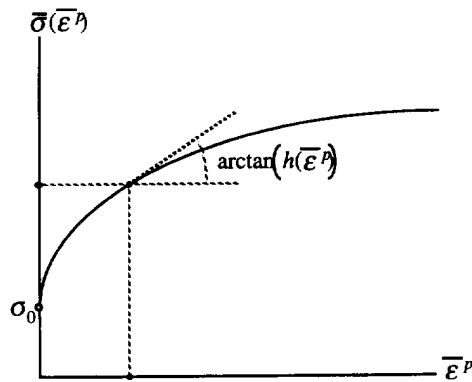
Fig. 1. Hardening function $\bar{\sigma}(\bar{\varepsilon}^p)$ and hardening slope $h(\bar{\varepsilon}^p)$.

and denote it by a superscript tilde. The transformed total strain $\tilde{\varepsilon}$ is deviatoric since it is the sum of the deviatoric transformed elastic strain $\tilde{\varepsilon}^e$ (2) and the deviatoric plastic strain $\varepsilon^p$, which obeys the incompressibility condition, $\varepsilon^p_{kk} = 0$, as shown below. Following Naghdi and Trapp (1975) we use a strain space description for our orthotropic plasticity model with the following set

$$v = (\tilde{\varepsilon}, \varepsilon^p, \bar{\varepsilon}^p)$$

of independent variables: the transformed (total) strain deviator $\tilde{\varepsilon}$, the plastic strain $\varepsilon^p$ and the equivalent plastic strain $\bar{\varepsilon}^p$ as the hardening parameter.

We introduce the hardening function $\bar{\sigma}(\bar{\varepsilon}^p)$ and its slope $h(\bar{\varepsilon}^p)$ by Fig. 1. The shear modulus is given by

$$G = \frac{1}{2}\frac{E}{1+v},$$

and $E$ and $v$ denote Young's modulus and Poisson's ratio, respectively. The total set of constitutive equations consists of:

● the yield function

$$g(v) = \|\tilde{\varepsilon} - \varepsilon^p\| - \sqrt{\frac{2}{3}}\frac{\bar{\sigma}(\bar{\varepsilon}^p)}{2G} = \|\tilde{\varepsilon}^e\| - \sqrt{\frac{2}{3}}\frac{\bar{\sigma}(\bar{\varepsilon}^p)}{2G}, \tag{11}$$

where the first term is the tensor norm

$$\|\tilde{\varepsilon}^e\| = \sqrt{\tilde{\varepsilon}^e_{ij}\tilde{\varepsilon}^e_{ji}} \tag{12}$$

of the transformed elastic strain (2) and the second term depends on the hardening parameter $\bar{\varepsilon}^p$;

● the flow rule

$$\dot{\varepsilon}^p = \begin{cases} 0 & \text{if } g < 0 & & \text{"elastic domain"} & (13a) \\ 0 & \text{if } g = 0 \text{ and } \overset{*}{g} < 0 & \text{"unloading"} & (13b) \\ 0 & \text{if } g = 0 \text{ and } \overset{*}{g} = 0 & \text{"neutral loading"} & (13c) \\ \dfrac{3G}{3G + h(\bar{\varepsilon}^p)}\mathbf{n}\overset{*}{g} & \text{if } g = 0 \text{ and } \overset{*}{g} > 0 & \text{"loading"} & (13d) \end{cases}$$

where

$$\mathbf{n} = \frac{\partial g}{\partial \tilde{\varepsilon}} = \frac{\hat{\varepsilon}^c}{\|\hat{\varepsilon}^c\|} \tag{14}$$

is the normal to the convex yield surface $g = 0$ in the transformed $\tilde{\varepsilon}$-space and $\overset{*}{g}$ is defined as

$$\overset{*}{g} = \frac{\partial g}{\partial \tilde{\varepsilon}_{kl}} \dot{\tilde{\varepsilon}}_{kl} = n_{lk} \dot{\tilde{\varepsilon}}_{kl} ;$$

● and the isotropic hardening law

$$\bar{\varepsilon}^P = \sqrt{2/3} n_{lk} \dot{\varepsilon}^P_{kl} = \sqrt{2/3} \|\dot{\varepsilon}^P\| . \tag{15}$$

Note, with eqns (11)–(15) the consistency condition

$$\dot{g} = \frac{\partial g}{\partial \tilde{\varepsilon}_{kl}} \dot{\tilde{\varepsilon}}_{kl} + \frac{\partial g}{\partial \varepsilon^P_{kl}} \dot{\varepsilon}^P_{kl} + \frac{\partial g}{\partial \bar{\varepsilon}^P} \dot{\bar{\varepsilon}}^P = 0$$

is fulfilled. Furthermore, the incompressibility condition of plastic strain

$$\varepsilon^P_{kk} = 0$$

follows from eqn (14) and the time integral of eqn (13). In a strain space description the stress is a dependent variable, which is not required for the description of plasticity, but which may be calculated using the isotropic stress–strain relation

$$\boldsymbol{\sigma} = 2G \left( \boldsymbol{\varepsilon} + \frac{v}{1-2v} \varepsilon_{kk} \mathbf{1} - \boldsymbol{\varepsilon}^P \right). \tag{16}$$

The tangential stiffness is calculated via the tangential elastic–plastic tensor which is defined by the time derivative of the stress–strain relations (16) with the flow rule (13) inserted. Within the framework of the finite deformation theory, $\boldsymbol{\sigma}$ is the logarithmic stress which is work-conjugate to the logarithmic strain rate $\dot{\boldsymbol{\varepsilon}}$. The tensors $\boldsymbol{\sigma}$ and $\dot{\boldsymbol{\varepsilon}}$ can be transformed to the Cauchy stress $\hat{\mathbf{T}}$ and the rate of deformation tensor $\hat{\mathbf{D}}$, respectively (Heiduschke, 1995, 1996).

The effect of the elastic strain transformation (2) is depicted in Fig. 2, where the orthotropic yield surface in the deviatoric plane of the principal $\varepsilon$-space (denoted vertically) is mapped into a von Mises cylinder in the deviatoric principal $\tilde{\varepsilon}$-space (10). A situation in
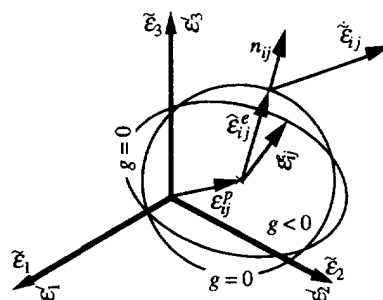


Fig. 2. The transformation of the elastic strain depicted in the deviatoric planes of the principal strain spaces of $\varepsilon$ and $\tilde{\varepsilon}$ denoted horizontally and vertically, respectively.

K. Heiduschke
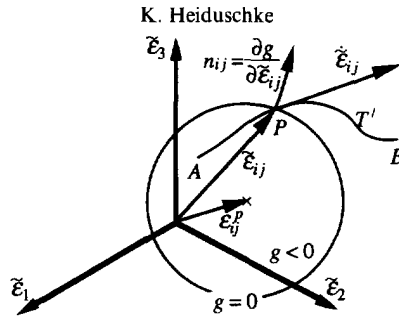


Fig. 3. Yield surface and its normal, strain trajectory, strain rate and plastic strain in the deviatoric principal ε̃-space.

the deviatoric principal ε̃-space is depicted in Fig. 3. The central axis of the von Mises cylinder is marked by the plastic strain $\varepsilon^p$. The transformed strain deviator ε̃ follows its trajectory $T'$ from $A$ to $B$. At the point $P$ the trajectory $T'$ hits the yield surface. From $P$ to $B$ plastic flow will occur and the yield surface must move, so that the strain ε̃ is always at the boundary $g = 0$. The material model prohibits the strain ε̃ from being outside the closed elastic domain ($g \leqslant 0$). The situation in Fig. 3 may be compared to: $g = 0$ is a ring, whose radius is dependent on the hardening parameter $\overline{\varepsilon^p}$. If we follow (draw) the trajectory from $A$ to $B$ with a pencil, the ring will be driven by the pencil beyond the point $P$. The total strain rate ε̃̇ is the tangent to the strain trajectory $T'$ and the normal to the yield surface n is parallel to the tensor difference (ε̃ − $\varepsilon^p$).

## 4. IDENTIFICATION OF THE ORTHOTROPY COEFFICIENTS BY $R$-VALUES

In order to identify the orthotropy coefficients $L$, $M$, $N$, $O$, $P$, $Q$ we define, according to Fig. 4, the following three-dimensional $r$-values for uniaxial tension in the:
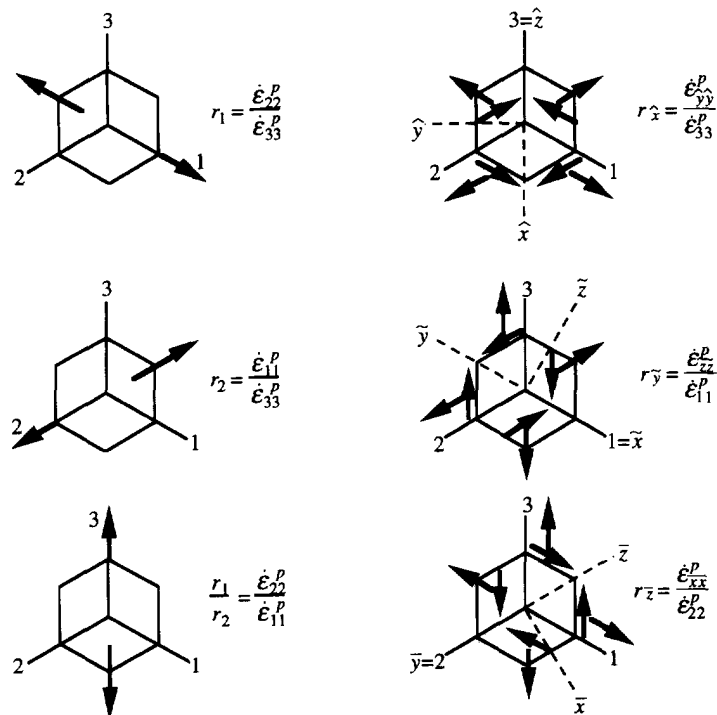


Fig. 4. Three-dimensional $r$-values defined by uniaxial tension along different material directions.

$$1\text{-direction } r_1 = \frac{\dot{\varepsilon}_{22}^p}{\dot{\varepsilon}_{33}^p}, \quad 2\text{-direction } r_2 = \frac{\dot{\varepsilon}_{11}^p}{\dot{\varepsilon}_{33}^p},$$

$$\hat{x}\text{-direction } r_{\hat{x}} = \frac{\dot{\varepsilon}_{\hat{y}\hat{y}}^p}{\dot{\varepsilon}_{33}^p}, \quad \tilde{y}\text{-direction } r_{\tilde{y}} = \frac{\dot{\varepsilon}_{\tilde{z}\tilde{z}}^p}{\dot{\varepsilon}_{11}^p}, \quad \bar{z}\text{-direction } r_{\bar{z}} = \frac{\dot{\varepsilon}_{\bar{x}\bar{x}}^p}{\dot{\varepsilon}_{22}^p}.$$

The $\hat{x}$-$\hat{y}$-axes (superscript hat), $\tilde{y}$-$\tilde{z}$-axes (superscript tilde) and $\bar{z}$-$\bar{x}$-axes (superscript bar) result from the 1-2-axes, 2-3-axes and 3-1-axes by a 45° rotation along 3, 1, and 2, respectively. For uniaxial tension in the 3-direction we have

$$\frac{r_1}{r_2} = \frac{\dot{\varepsilon}_{22}^p}{\dot{\varepsilon}_{11}^p}.$$

The stress components associated with the six uniaxial tension cases of Fig. 4 are given by the first column of Table 1, entitled $\sigma_{ij}$. The corresponding equivalent flow stresses $\bar{\sigma}$ of the hardening function are given in column two. They follow from the elastic strain components $\varepsilon_{ij}^e$ of column three, via $\sigma_{ij}$ and the inverse of (16), from the transformed elastic strain $\hat{\varepsilon}_{ij}^e$ of column four, via $\varepsilon_{ij}^e$ and the deviator transformation (2) and from the norm (12) of the transformed elastic strain $\|\hat{\varepsilon}^e\|$ in column five. The plastic flow $\dot{\varepsilon}_{ij}^p$ in column six is parallel to $\hat{\varepsilon}_{ij}^e$ according to the flow rule (13). Its norm $\|\dot{\varepsilon}^p\|$ in column seven is the equivalent plastic strain increment (15) multiplied by $\sqrt{3/2}$.

For the cases of uniaxial tension under 45° to the principal material directions (rows four to six of Table 1) we rotate the 1-, 2-, 3-co-ordinate systems by 45° along the 3-, 1- and 2-axes and express the components of the plastic flow tensors (column six) in the $\hat{x}$-$\hat{y}$-3-, 1-$\tilde{y}$-$\tilde{z}$- and $\bar{x}$-2-$\bar{z}$-bases by

$$\dot{\varepsilon}_{ij}^p = \begin{bmatrix} N+L+6O & N-L & 0 \\ N-L & N+L-6O & 0 \\ 0 & 0 & -2(N+L) \end{bmatrix} \frac{3\dot{\sigma}_4}{8h},$$

$$\dot{\varepsilon}_{ij}^p = \begin{bmatrix} -2(L+M) & 0 & 0 \\ 0 & L+M+6P & L-M \\ 0 & L-M & L+M-6P \end{bmatrix} \frac{3\dot{\sigma}_5}{8h}$$

and

$$\dot{\varepsilon}_{ij}^p = \begin{bmatrix} M+N-6Q & 0 & M-N \\ 0 & -2(M+N) & 0 \\ M-N & 0 & M+N+6Q \end{bmatrix} \frac{3\dot{\sigma}_6}{8h},$$

respectively. Therefore, the three-dimensional $r$-values of Fig. 4 are

$$r_1 = \frac{M}{L}, \quad r_2 = \frac{M}{N}, \quad r_{\hat{x}} = \frac{3O}{N+L} - \frac{1}{2}, \quad r_{\tilde{y}} = \frac{3P}{L+M} - \frac{1}{2}, \quad r_{\bar{z}} = \frac{3Q}{M+N} - \frac{1}{2}.$$

By inverting the above equations we find the orthotropy coefficients

Table 1. Yielding of the proposed model in uniaxial tensile tests along the material direction 1, 2, 3, $\hat{x}$, $\hat{y}$, $\hat{z}$

| $\sigma_{ij}$ | $\bar{\sigma}$ | $\varepsilon_{ij}^{e}$ | $\bar{\varepsilon}_{ij}^{e}$ | $\|\hat{\varepsilon}^{e}\|$ | $\dot{\varepsilon}_{ij}^{p}$ | $\|\dot{\hat{\varepsilon}}^{p}\|$ |
|---|---|---|---|---|---|---|
| $\begin{bmatrix}1&0&0\\0&0&0\\0&0&0\end{bmatrix}\sigma_1$ | $\sigma_1\sqrt{3(L^2+LM+M^2)}$ | $\begin{bmatrix}1&0&0\\0&-v&0\\0&0&-v\end{bmatrix}\dfrac{\sigma_1}{E}$ | $\begin{bmatrix}L+M&0&0\\0&-M&0\\0&0&-L\end{bmatrix}\dfrac{\sigma_1}{2G}$ | $\dfrac{\bar{\sigma}}{\sqrt{6}G}$ | $\begin{bmatrix}L+M&0&0\\0&-M&0\\0&0&-L\end{bmatrix}\dfrac{3\dot{\sigma}_1}{2h}$ | $\sqrt{\dfrac{3}{2}}\dfrac{\dot{\bar{\sigma}}}{h}$ |
| $\begin{bmatrix}0&0&0\\0&1&0\\0&0&0\end{bmatrix}\sigma_2$ | $\sigma_2\sqrt{3(M^2+MN+N^2)}$ | $\begin{bmatrix}-v&0&0\\0&1&0\\0&0&-v\end{bmatrix}\dfrac{\sigma_2}{E}$ | $\begin{bmatrix}-M&0&0\\0&M+N&0\\0&0&-N\end{bmatrix}\dfrac{\sigma_2}{2G}$ | $\dfrac{\bar{\sigma}}{\sqrt{6}G}$ | $\begin{bmatrix}-M&0&0\\0&M+N&0\\0&0&-N\end{bmatrix}\dfrac{3\dot{\sigma}_2}{2h}$ | $\sqrt{\dfrac{3}{2}}\dfrac{\dot{\bar{\sigma}}}{h}$ |
| $\begin{bmatrix}0&0&0\\0&0&0\\0&0&1\end{bmatrix}\sigma_3$ | $\sigma_3\sqrt{3(N^2+NL+L^2)}$ | $\begin{bmatrix}-v&0&0\\0&-v&0\\0&0&1\end{bmatrix}\dfrac{\sigma_3}{E}$ | $\begin{bmatrix}-L&0&0\\0&-N&0\\0&0&N+L\end{bmatrix}\dfrac{\sigma_3}{2G}$ | $\dfrac{\bar{\sigma}}{\sqrt{6}G}$ | $\begin{bmatrix}-L&0&0\\0&-N&0\\0&0&N+L\end{bmatrix}\dfrac{3\dot{\sigma}_3}{2h}$ | $\sqrt{\dfrac{3}{2}}\dfrac{\dot{\bar{\sigma}}}{h}$ |
| $\begin{bmatrix}1&1&0\\1&1&0\\0&0&0\end{bmatrix}\dfrac{\sigma_4}{2}$ | $\dfrac{\sigma_4\sqrt{3(N^2+NL+L^2+9O^2)}}{2}$ | $\begin{bmatrix}1-v&1+v&0\\1+v&1-v&0\\0&0&-2v\end{bmatrix}\dfrac{\sigma_4}{2E}$ | $\begin{bmatrix}L&3O&0\\3O&N&0\\0&0&-N-L\end{bmatrix}\dfrac{\sigma_4}{4G}$ | $\dfrac{\bar{\sigma}}{\sqrt{6}G}$ | $\begin{bmatrix}L&3O&0\\3O&N&0\\0&0&-N-L\end{bmatrix}\dfrac{3\dot{\sigma}_4}{4h}$ | $\sqrt{\dfrac{3}{2}}\dfrac{\dot{\bar{\sigma}}}{h}$ |
| $\begin{bmatrix}0&0&0\\0&1&1\\0&1&1\end{bmatrix}\dfrac{\sigma_5}{2}$ | $\dfrac{\sigma_5\sqrt{3(L^2+LM+M^2+9P^2)}}{2}$ | $\begin{bmatrix}-2v&0&0\\0&1-v&1+v\\0&1+v&1-v\end{bmatrix}\dfrac{\sigma_5}{2E}$ | $\begin{bmatrix}-L-M&0&0\\0&M&3P\\0&3P&L\end{bmatrix}\dfrac{\sigma_5}{4G}$ | $\dfrac{\bar{\sigma}}{\sqrt{6}G}$ | $\begin{bmatrix}-L-M&0&0\\0&M&3P\\0&3P&L\end{bmatrix}\dfrac{3\dot{\sigma}_5}{4h}$ | $\sqrt{\dfrac{3}{2}}\dfrac{\dot{\bar{\sigma}}}{h}$ |
| $\begin{bmatrix}1&0&1\\0&0&0\\1&0&1\end{bmatrix}\dfrac{\sigma_6}{2}$ | $\dfrac{\sigma_6\sqrt{3(M^2+MN+N^2+9Q^2)}}{2}$ | $\begin{bmatrix}1-v&0&1+v\\0&-2v&0\\1+v&0&1-v\end{bmatrix}\dfrac{\sigma_6}{2E}$ | $\begin{bmatrix}M&0&3Q\\0&-M-N&0\\3Q&0&N\end{bmatrix}\dfrac{\sigma_6}{4G}$ | $\dfrac{\bar{\sigma}}{\sqrt{6}G}$ | $\begin{bmatrix}M&0&3Q\\0&-M-N&0\\3Q&0&N\end{bmatrix}\dfrac{3\dot{\sigma}_6}{4h}$ | $\sqrt{\dfrac{3}{2}}\dfrac{\dot{\bar{\sigma}}}{h}$ |

$$L = \frac{\lambda}{r_1}, \quad M = \lambda, \quad N = \frac{\lambda}{r_2}, \quad O = \frac{\lambda}{6}(1 + 2r_x)\left(\frac{1}{r_1} + \frac{1}{r_2}\right),$$

$$P = \frac{\lambda}{6}(1 + 2r_y)\left(1 + \frac{1}{r_1}\right), \quad Q = \frac{\lambda}{6}(1 + 2r_z)\left(1 + \frac{1}{r_2}\right),$$

where $\lambda$ is a free parameter which corresponds to the scalar weighting of the hardening function. Without loss of generality we set $\lambda = 1/3$ so that (9) is fulfilled. Hence, the orthotropy coefficients are

$$L = \frac{1}{3r_1}, \quad M = \frac{1}{3}, \quad N = \frac{1}{3r_2},$$

$$O = \frac{1}{18}(1 - 2r_x)\left(\frac{1}{r_1} + \frac{1}{r_2}\right), \quad P = \frac{1}{18}(1 + 2r_y)\left(1 + \frac{1}{r_1}\right), \quad Q = \frac{1}{18}(1 + 2r_z)\left(1 + \frac{1}{r_2}\right). \quad (17)$$

For a co-ordinate system oriented with the $z$-axis pointing in the thickness direction of sheet metal the above $r$-values are related with the usual $R_{0^\circ}$, $R_{45^\circ}$, $R_{90^\circ}$-values by

$$R_0 = r_1, \quad R_{45} = r_x, \quad R_{90} = r_2. \quad (18)$$

Furthermore, for transverse isotropy of sheet metal characterised by $R = R_0 = R_{45^\circ} = R_{90}$ the deviator transformation (2) becomes invariant to rotations in the sheet metal plane

$$\omega'_{ijkl} = Q_{im}Q_{jn}Q_{ko}Q_{lp}\omega_{mnop} \quad \text{with } Q_{im} = \begin{bmatrix} \cos\varphi & -\sin\varphi & 0 \\ \sin\varphi & \cos\varphi & 0 \\ 0 & 0 & 1 \end{bmatrix},$$

so that

$$\omega'_{ijkl} = \omega_{ijkl}$$

holds.



Fig. 5. The partly skew-symmetric shear deformation of 45° specimens under uniaxial tension.

The experimental determination of $r$-values with standard tensile tests may appear surprising. For orthotropic sheet metal with $R_0 \neq R_{90}$ the directions of 45° to the principal material axes are no planes of material symmetry. If, therefore, a uniaxial tensile load is applied to a 45°-specimen a combination of shear and tensile deformation results, as depicted in Fig. 5. This partly skew-symmetric shear deformation causes problems with the tensile test set-up, since it disturbs the homogeneity of the investigated deformation field. However, 45°-tensile tests on commercially available sheet metal, Hoesch and Krupp (1992), do not exhibit the behavior shown in Fig. 5. The 45°-material directions seems to be planes of symmetry in most of the sheet metal used in production with the corresponding $R$-values $R_0 = R_{90}$.

## 5. COMPARISON WITH HILL'S MODEL

Hill (1948) originally specified his yield function in the stress space (Hill, 1979). For a comparison of the present model with Hill (1979) we rewrite Hill's yield function in our notation

$$f_{\text{HILL}}(\boldsymbol{\sigma}, \overline{\varepsilon_{\text{HILL}}^{\text{p}}}) = \sqrt{\sigma_{ij}\omega_{ijkl}\sigma_{kl}} - \sqrt{\tfrac{2}{3}}\bar{\sigma}(\overline{\varepsilon_{\text{HILL}}^{\text{p}}}), \tag{19}$$

where

$$\overline{\dot{\varepsilon}_{\text{HILL}}^{\text{p}}} = \sqrt{\tfrac{2}{3}\dot{\varepsilon}_{ij}^{\text{p}}\rho_{ijkl}\dot{\varepsilon}_{kl}^{\text{p}}} \tag{20}$$

denotes Hill's definition of equivalent plastic strain. Using the features (4) of the deviator transformation (2) and the deviatoric stress–strain relation

$$\boldsymbol{\sigma}' = 2G\boldsymbol{\varepsilon}'^{\text{e}}, \tag{21}$$

we express our yield function (11) as

$$f(\boldsymbol{\sigma}, \bar{\varepsilon}^{\text{p}}) = \sqrt{\sigma_{ij}\omega_{ijkl}\omega_{klmn}\sigma_{mn}} - \sqrt{\tfrac{2}{3}}\bar{\sigma}(\bar{\varepsilon}^{\text{p}}), \tag{22}$$

which may be compared† with (19). The orthotropy coefficients of $\omega$ used in both models are compiled in Table 2. It should be noted that even if the yield functions (19) and (22) are different, the normal tensors used in the constitutive models are parallel, denoted by $\sim$,

$$\mathbf{n}_{\text{HILL}} \sim \mathbf{n} \sim \omega\boldsymbol{\sigma} \sim \omega\boldsymbol{\varepsilon}^{\text{e}} \sim \dot{\boldsymbol{\varepsilon}}^{\text{p}},$$

where $\mathbf{n}_{\text{HILL}}$ and $\mathbf{n}$ are the normal tensor to Hill's yield function (19) in the original $\varepsilon$-space and the normal tensor (14) to the yield function (11) in the transformed $\bar{\varepsilon}$-space, respectively.

Hill's and the model presented are compared for a uniaxial tension load in the material directions depicted in Fig. 4. The material response of Hill's model is given in Table 3, which is analogous to Table 1 of the present model. Column four of Table 3 lists the first term of Hill's yield function

$$g_{\text{HILL}}(v) = \sqrt{\varepsilon_{ij}'^{\text{e}}\omega_{ijkl}\varepsilon_{kl}'^{\text{e}}} - \sqrt{\tfrac{2}{3}}\frac{\bar{\sigma}(\overline{\varepsilon_{\text{HILL}}^{\text{p}}})}{2G},$$

which corresponds to the first term of (11). Column six of Table 3 lists Hill's equivalent plastic strain increment (20) multiplied by $\sqrt{3/2}$, which may be compared to $\|\dot{\boldsymbol{\varepsilon}}^{\text{p}}\|$ of the present model compiled in Table 1. Hill's hardening law is termed strain- and work-hardening, as Hill's equivalent plastic strain increment as well as the plastic dissipation

$$\sigma_{ij}\dot{\varepsilon}_{ij}^{\text{p}} = \bar{\sigma}\overline{\dot{\varepsilon}_{\text{HILL}}^{\text{p}}}$$

are constant for different material directions, Table 3. On the other hand, the hardening law of the model presented exhibits strain-hardening behavior. Only the equivalent plastic strain increment is constant for different material directions, the plastic dissipation $\sigma_{ij}\dot{\varepsilon}_{ij}^{\text{p}}$ is not.

Table 2. Designation of the orthotropy coefficients

| Hill (1979) | $\beta$ | $g$ | $h$ | $f$ | $n$ | $l$ | $m$ |
|---|---|---|---|---|---|---|---|
| Present model | $\omega$ | $L$ | $M$ | $N$ | $3O$ | $3P$ | $3Q$ |

† Note the non-equivalence of loading conditions of stress and strain space descriptions for the finite deformation theory as pointed out by Casey and Naghdi (1983), Moss (1984) and Naghdi (1990).

Table 3. Yielding of Hill's model in uniaxial tensile tests along the material directions 1, 2, 3, $\hat{x}$, $\hat{y}$, $\hat{z}$

| $\sigma_{ij}$ | $\bar{\sigma}$ | $\varepsilon_{ij}^e$ | $\sqrt{\varepsilon_{ij}^e \omega_{ijkl} \varepsilon_{kl}^e}$ | $\varepsilon_{ij}^p$ | $\sqrt{\varepsilon_{ij}^p \rho_{ijkl} \varepsilon_{kl}^p}$ |
|---|---|---|---|---|---|
| $\begin{bmatrix} 1 & 0 & 0 \\ 0 & 0 & 0 \\ 0 & 0 & 0 \end{bmatrix}\sigma_1$ | $\sqrt{\frac{3}{2}}\sigma_1\sqrt{L+M}$ | $\begin{bmatrix} 1 & 0 & 0 \\ 0 & -v & 0 \\ 0 & 0 & -v \end{bmatrix}\frac{\sigma_1}{E}$ | $\dfrac{\bar{\sigma}}{\sqrt{6}G}$ | $\begin{bmatrix} L+M & 0 & 0 \\ 0 & -M & 0 \\ 0 & 0 & -L \end{bmatrix}\frac{3\dot{\sigma}_1}{2h}$ | $\sqrt{\frac{3}{2}}\dfrac{\dot{\bar{\sigma}}}{h}$ |
| $\begin{bmatrix} 0 & 0 & 0 \\ 0 & 1 & 0 \\ 0 & 0 & 0 \end{bmatrix}\sigma_2$ | $\sqrt{\frac{3}{2}}\sigma_2\sqrt{M+N}$ | $\begin{bmatrix} -v & 0 & 0 \\ 0 & 1 & 0 \\ 0 & 0 & -v \end{bmatrix}\frac{\sigma_2}{E}$ | $\dfrac{\bar{\sigma}}{\sqrt{6}G}$ | $\begin{bmatrix} -M & 0 & 0 \\ 0 & M+N & 0 \\ 0 & 0 & -N \end{bmatrix}\frac{3\dot{\sigma}_2}{2h}$ | $\sqrt{\frac{3}{2}}\dfrac{\dot{\bar{\sigma}}}{h}$ |
| $\begin{bmatrix} 0 & 0 & 0 \\ 0 & 0 & 0 \\ 0 & 0 & 1 \end{bmatrix}\sigma_3$ | $\sqrt{\frac{3}{2}}\sigma_3\sqrt{N+L}$ | $\begin{bmatrix} -v & 0 & 0 \\ 0 & -v & 0 \\ 0 & 0 & 1 \end{bmatrix}\frac{\sigma_3}{E}$ | $\dfrac{\bar{\sigma}}{\sqrt{6}G}$ | $\begin{bmatrix} -L & 0 & 0 \\ 0 & N & 0 \\ 0 & 0 & N+L \end{bmatrix}\frac{3\dot{\sigma}_3}{2h}$ | $\sqrt{\frac{3}{2}}\dfrac{\dot{\bar{\sigma}}}{h}$ |
| $\begin{bmatrix} 1 & 1 & 0 \\ 1 & 1 & 0 \\ 0 & 0 & 0 \end{bmatrix}\frac{\sigma_4}{2}$ | $\sqrt{\frac{3}{8}}\sigma_4\sqrt{N+L+6O}$ | $\begin{bmatrix} 1-v & 1+v & 0 \\ 1+v & 1-v & 0 \\ 0 & 0 & -2v \end{bmatrix}\frac{\sigma_4}{2E}$ | $\dfrac{\bar{\sigma}}{\sqrt{6}G}$ | $\begin{bmatrix} L & 3O & 0 \\ 3O & N & 0 \\ 0 & 0 & -N-L \end{bmatrix}\frac{3\dot{\sigma}_4}{4h}$ | $\sqrt{\frac{3}{2}}\dfrac{\dot{\bar{\sigma}}}{h}$ |
| $\begin{bmatrix} 0 & 0 & 0 \\ 0 & 1 & 1 \\ 0 & 1 & 1 \end{bmatrix}\frac{\sigma_5}{2}$ | $\sqrt{\frac{3}{8}}\sigma_5\sqrt{L+M+6P}$ | $\begin{bmatrix} -2v & 0 & 0 \\ 0 & 1-v & 1+v \\ 0 & 1+v & 1-v \end{bmatrix}\frac{\sigma_5}{2E}$ | $\dfrac{\bar{\sigma}}{\sqrt{6}G}$ | $\begin{bmatrix} -L-M & 0 & 0 \\ 0 & M & 3P \\ 0 & 3P & L \end{bmatrix}\frac{3\dot{\sigma}_5}{4h}$ | $\sqrt{\frac{3}{2}}\dfrac{\dot{\bar{\sigma}}}{h}$ |
| $\begin{bmatrix} 1 & 0 & 1 \\ 0 & 0 & 0 \\ 1 & 0 & 1 \end{bmatrix}\frac{\sigma_6}{2}$ | $\sqrt{\frac{3}{8}}\sigma_6\sqrt{M+N+6Q}$ | $\begin{bmatrix} 1-v & 0 & 1+v \\ 0 & -2v & 0 \\ 1+v & 0 & 1-v \end{bmatrix}\frac{\sigma_6}{2E}$ | $\dfrac{\bar{\sigma}}{\sqrt{6}G}$ | $\begin{bmatrix} M & 0 & 3Q \\ 0 & -M-N & 0 \\ 3Q & 0 & N \end{bmatrix}\frac{3\dot{\sigma}_6}{4h}$ | $\sqrt{\frac{3}{2}}\dfrac{\dot{\bar{\sigma}}}{h}$ |

## 6. THERMODYNAMICAL RESTRICTIONS

From thermodynamical considerations and, especially, the second law, the constitutive restriction

$$\oint \sigma_{ij}\, d\varepsilon^{p}_{ij} = \oint \sigma_{ij}\dot{\varepsilon}^{p}_{ij}\, dt \geqslant 0,\tag{23}$$

which must hold for arbitrary work cycles, has been derived by Naghdi and Trapp (1975) within the framework of the finite deformation theory.† The restriction (23), also termed the non-negativity of work cycles assumption of Drucker and Prager, is fulfilled if

$$\sigma_{ij}\dot{\varepsilon}^{p}_{ij} \geqslant 0$$

holds. For elasticity (13a), unloading from a plastic state (13b) or neutral loading (13c) we have

$$\sigma_{ij}\dot{\varepsilon}^{p}_{ij} = 0.$$

For loading into a plastic state we rewrite (13d) by use of (2) and (14) as

$$\dot{\varepsilon}^{p}_{ij} = \frac{3G}{3G+h(\bar{\varepsilon}^{p})}\frac{\omega_{ijkl}\dot{\varepsilon}^{e}_{kl}}{|\dot{\varepsilon}^{e}|}\overset{*}{g}.\tag{24}$$

Since $\dot{\varepsilon}^{p}$ is deviatoric we have $\sigma_{ij}\dot{\varepsilon}^{p}_{ij} = \sigma'_{ij}\dot{\varepsilon}^{p}_{ij}$ and from eqns (4) and (5) $\omega_{ijkl}\dot{\varepsilon}^{e}_{kl} = \omega_{ijkl}\dot{\varepsilon}'^{e}_{kl}$. Finally, using (24) we find for plastic loading that

$$\sigma_{ij}\dot{\varepsilon}^{p}_{ij} = \frac{3/2}{3G+h(\bar{\varepsilon}^{p})}\frac{\sigma'_{ij}\omega_{ijkl}\sigma'_{kl}}{|\dot{\varepsilon}^{e}|}\overset{*}{g} > 0$$

is greater than zero, since $3G+h(\bar{\varepsilon}^{p}) > 0$, $\sigma'_{ij}\omega_{ijkl}\sigma'_{kl} = \sigma_{ij}\omega_{ijkl}\sigma_{kl} > 0$, eqn (19), $|\dot{\varepsilon}^{e}| > 0$, by definition (12) and $\overset{*}{g} > 0$, (13d). Hence, the presented model fulfils the thermodynamical restriction (23) for arbitrary work cycles.

## 7. ALGORITHMIC ASPECTS

For the time discretization the current time step is denoted by a top left index and the increment between two consecutive time steps by a prescript $\Delta$. Hence, the discretized strain increment is

$$\Delta\varepsilon = {}^{t+1}\varepsilon - {}^{t}\varepsilon.$$

Furthermore, the hardening function of Fig. 1 is approximated piecewise linearly. Following Heiduschke and Sayir (1989), Heiduschke (1990) and Heiduschke et al. (1991) the discretization of the flow rule (13) is given by

$$\Delta\varepsilon^{p} = (1-\Omega)\frac{3G}{3G+h({}^{t}\bar{\varepsilon}^{p})}({}^{t+1}\bar{\varepsilon} - {}^{t}\bar{\varepsilon}^{p})\tag{25}$$

with the inverse outside factor

---

† As pointed out by Naghdi and Trapp (1975), the restriction (23) should not be confused with the postulate of Drucker (1952, 1964), which has only been formulated within the infinitesimal deformation theory.

$$\Omega = \frac{\sqrt{\dfrac{2}{3}\,\dfrac{\bar{\sigma}('\varepsilon^{\mathrm{p}})}{2G}}}{\|\,^{t+1}\tilde{\varepsilon} - {}^t\varepsilon^{\mathrm{p}}\,\|}, \tag{26}$$

with the hardening function $\bar{\sigma}('\varepsilon^{\mathrm{p}})$, its slope $h('\varepsilon^{\mathrm{p}})$ as depicted by Fig. 1 and with $\|\cdot\|$ denoting the tensor norm (12). Within the infinitesimal deformation theory, the time-discretization formulas (25) and (26) are identical with the strain-space version of the radial return method of Krieg and Krieg (1977), also with respect to consistency, stability and accuracy. The strain difference on the right hand side of (25) may be rewritten as

$$^{t+1}\tilde{\varepsilon} - {}^t\varepsilon^{\mathrm{p}} = \omega^{t+1}\varepsilon^{\mathrm{e}} + \Delta\varepsilon^{\mathrm{p}} \quad \text{with } ^{t+1}\varepsilon^{\mathrm{e}} = (^{t+1}\varepsilon - {}^t\varepsilon^{\mathrm{p}}) - \Delta\varepsilon^{\mathrm{p}}. \tag{27}$$

Using (27) the discretized flow rule (25) is expressed by the inverse outside factor $\Omega$ and the difference of the new total strain minus the old plastic strain

$$\Delta\varepsilon^{\mathrm{p}} = (1-\Omega)\left[\left(\frac{h('\bar{\varepsilon}^{\mathrm{p}})}{3G} + \Omega\right)\mathbf{1}' + (1-\Omega)\omega\right]^{-1'} \omega(^{t+1}\varepsilon - {}^t\varepsilon^{\mathrm{p}}), \tag{28}$$

where $\mathbf{1}'$ denotes the deviatoric fourth-order unit tensor and $[\cdot]^{-1'}$ the deviatoric inverse fourth-order tensor which is defined via eqns (7), (8). The inverse outside factor $\Omega$ is determined in the constitutive algorithm by the numerical solution of the scalar polynomial

$$p_0 + p_1\Omega + p_2\Omega^2 + p_3\Omega^3 + \cdots + p_9\Omega^9 + p_{10}\Omega^{10} = 0, \tag{29}$$

which follows from squaring eqn (26) and inserting eqns (27) and (28). The coefficients

$$p_i = p_i(^{t+1}\varepsilon, {}^t\varepsilon^{\mathrm{p}}, {}^t\bar{\varepsilon}^{\mathrm{p}}) \tag{30}$$

are functions of the time-dependent variables $^{t+1}\varepsilon$, ${}^t\varepsilon^{\mathrm{p}}$, ${}^t\bar{\varepsilon}^{\mathrm{p}}$ and of the material parameters $G$, $\bar{\sigma}('\varepsilon^{\mathrm{p}})$, $h('\bar{\varepsilon}^{\mathrm{p}})$, $L$, $M$, $N$, $O$, $P$ and $Q$. The calculation of the $p_i$-coefficients (29) is rather involved and only manageable by using a symbolic algebra program, like Mathematica of Wolfram (1991). In the discretized constitutive model plastic flow occurs only if the total strain of the current time step lies outside the yield surface of the previous step. The inverse outside factor $\Omega$, which is defined as the quotient of the previous radius to the current trial radius of the von Mises cylinder in the transformed strain space $\tilde{\varepsilon}$, obeys

$$1 > \Omega > 0, \tag{31}$$

and the polynomial (29) has only one real solution in the interval (31). Once the inverse outside factor $\Omega$ is determined numerically from eqns (29)–(31) the plastic flow increment follows directly from eqn (28), without iterations on tensor quantities. The hardening parameter $'\bar{\varepsilon}^{\mathrm{p}}$ is given by the time-integrated norm of $\Delta\varepsilon^{\mathrm{p}}$ (15), the stress $\sigma$ by the stress-strain relations (16) and the tangential elastic-plastic matrix by the time derivative of the stress-strain relations (16) with the flow rule (13) inserted.

## 8. SIMULATION RESULTS ON EARING OF SHEET METAL

A specially designed version of our constitutive model is implemented in the finite element program AutoForm which simulates the forming process of sheet metal. The isotropic algorithm has been presented by Heiduschke et al. (1991). The sheet metal is modelled by plane triangular membrane elements. It is described in a co-ordinate system co-rotating with respect to the membrane elements with the $z$-axis pointing in the thickness direction. Hence, the $yz$- and $zx$-components of the relevant stress and strain tensors vanish and the constitutive algorithm is driven by the following set of load parameters

$$^{t+1}\varepsilon_{xx}, \quad {}^{t+1}\varepsilon_{xy}, \quad {}^{t+1}\varepsilon_{yy}, \quad {}^{t+1}\sigma_{zz}, \tag{32}$$

namely the strain tensor components in the sheet plane and the stress component normal to it, which is determined from the downholder pressure. Using the $zz$-component of eqn (16) the driving tensor difference, ${}^{t+1}\varepsilon - {}'\varepsilon^p$, on the right-hand-side of eqn (28) may be rewritten for the set (32) of constitutive load parameters. With (32) the relevant orthotropy coefficients (17) reduce to

$$L = \frac{1}{3R_0}, \quad M = \frac{1}{3}, \quad N = \frac{1}{3R_{90}}, \quad O = \frac{1}{18}(1+2R_{45})\left(\frac{1}{R_0} + \frac{1}{R_{90}}\right). \tag{33}$$

The deformation, strains and rotations encountered in sheet metal forming processes are moderate. Therefore, the constitutive description is based on the logarithmic strain space, i.e. on the logarithmic strain $\varepsilon$ and the work-conjugate logarithmic stress $\sigma$ with respect to the reference configuration. In order to derive the finite element stiffness matrices and equivalent nodal forces, which are required for the global system of nonlinear equilibrium equations, the tensors $\varepsilon$ and $\sigma$ are respectively transformed (Heiduschke, 1995) to the rate of deformation tensor $\hat{D}$ and the Cauchy stress $\hat{T}$ with respect to the current configuration, where the principle of virtual work is applied. The global system solution, which can be decoupled into bending and stretching (Kubli, 1991, 1995) is achieved using Newton–Raphson iterations on the current node positions. This iterative global solution procedure should not be confused with the explicitness of the constitutive algorithm presented in this study. In an explicit constitutive algorithm the constitutive tensors are not iterated.

An interesting consequence of orthotropic material behavior is the earing effect, which we study in the example of the deep drawing of circular sheet metal under a spherical punch. For reasons of material and geometrical symmetry we model only one quarter of the sheet shown in Fig. 6. The initially flat sheet metal of Fig. 6 is deep drawn. Its deformed shape is depicted in the isometric view of Fig. 7.

The earing effect is best visible with a top view, as shown in Fig. 6 for the initial shape and in Figs 8–10 for the deformed shapes. The sets of $R$-values

$$R_0 = R_{45} = R_{90} = 1, \tag{34}$$

$$R_0 = 2, \quad R_{45} = R_{90} = 1, \tag{35}$$

$$R_{45} = 2, \quad R_0 = R_{90} = 1, \tag{36}$$

as defined in Fig. 4 and eqns (18), (33) correspond to the Figs 8–10, respectively. Isotropic
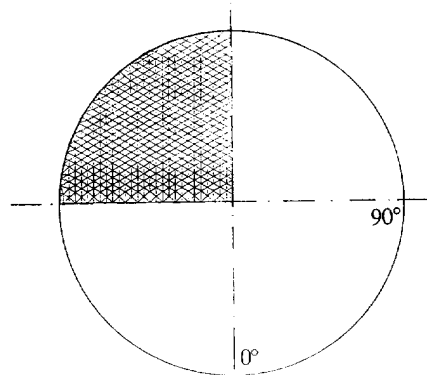


Fig. 6. Top view of a flat circular sheet metal with planes of symmetry and the initial finite element mesh.
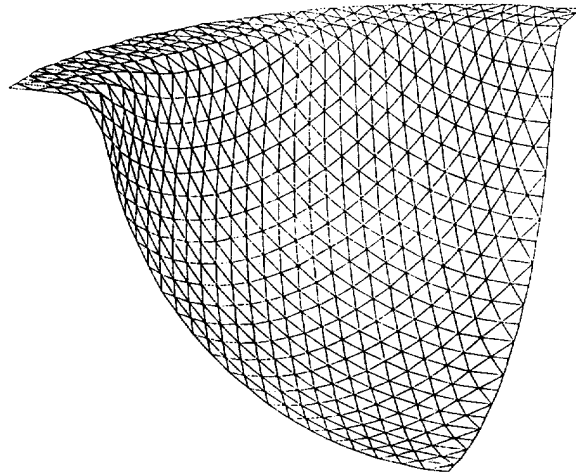
Fig. 7. Isometric view of the deformed finite element mesh resulting
from deep drawing with a spherical punch.
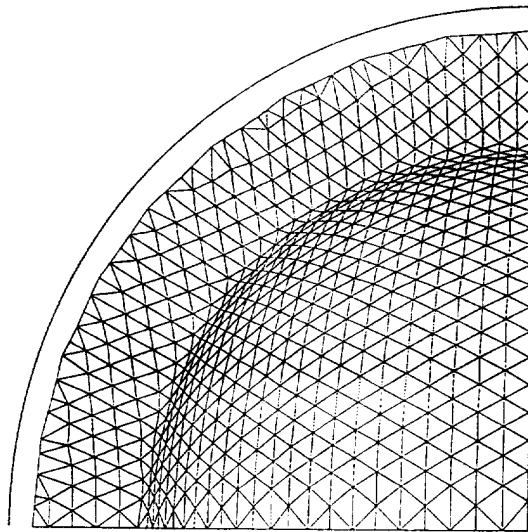


Fig. 8. Top view of the deformed finite element mesh for isotropy (34).
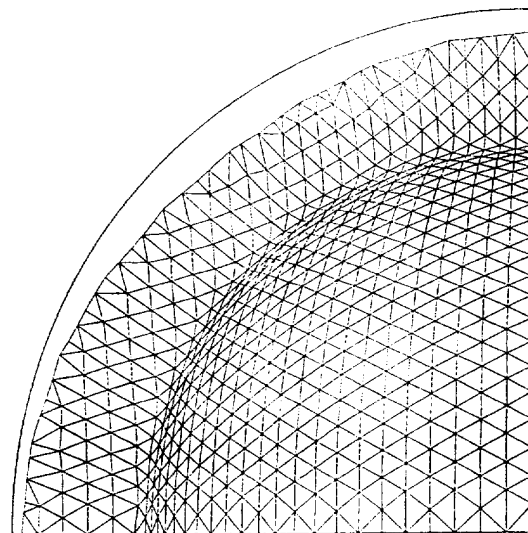


Fig. 9. Top view of the deformed finite element mesh for orthotropy
with respect to a normal component (35).
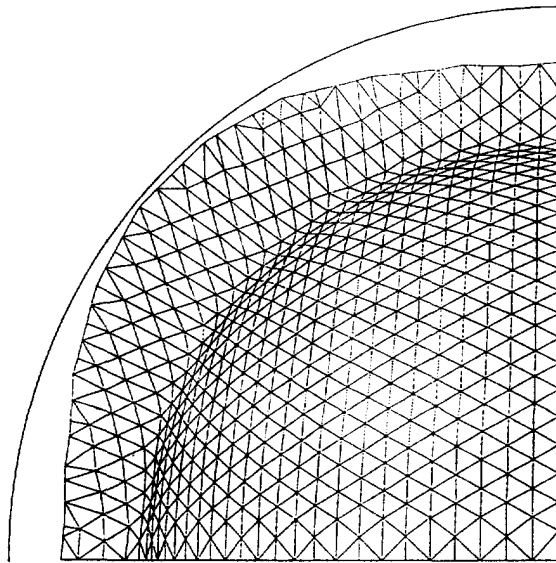
Fig. 10. Top view of the deformed finite element mesh for orthotropy with respect to a shear
component (36).

material behavior (34) is depicted in Fig. 8 and results in a circular shape. For orthotropy
with respect to a normal component (35) the deformed shape shown in Fig. 9 has two ears
and is similar to an ellipse. For orthotropy with respect to a shear component (36) four
ears result, as depicted in Fig. 10. The case (35) of Fig. 9 is interesting: compared to
isotropy (34) the $R_0$-value is increased, but the ears appear in the 90°-direction. This effect
is in accordance with (33), where the shear coefficient $O$ is proportional to the $R_{45}$-value
and where the normal coefficients $L$ and $N$ are inversely proportional to $R_0$ and $R_{90°}$,
respectively.

## 9. CONCLUSIONS

The presented constitutive model for isotropic elasticity and orthotropic plasticity is
based on the deviator transformation (2) of the elastic portion of the strain (1). It transforms
the orthotropic yield function of the original strain space $\varepsilon$ to an isotropic yield function in
a transformed strain space $\tilde{\varepsilon}$, where the strain space equivalent of the radial return method
of Krieg and Krieg (1977) is applied.

Radial return is a method of stress space descriptions. In the deviatoric plane of the
stress space, the amount of radial return is given by the plastic strain increment multiplied
by $2G$. In the corresponding strain space algorithms the whole yield function is, on the
other hand, shifted by the plastic strain increment. For the infinitesimal deformation theory,
where stress space and strain space descriptions are identical, the radial return method and
the corresponding strain space algorithm are identical, also with respect to accuracy,
stability and consistency. However, for the finite deformation theory the stress space and
strain space descriptions are no longer equivalent (Casey and Naghdi, 1983; Moss, 1984;
Naghdi, 1990) since the underlying stress and strain definitions differ. Hence, the physical
behavior of the corresponding constitutive models is also different.

The combination of the dev.ator transformation and the strain space version of the
radial return method yields an explicit constitutive algorithm which requires no iterations
on constitutive tensors. Therefore, the algorithm's vector performance is excellent, about
3% slower than the isotropic elastic–plastic algorithm of Heiduschke et al. (1991), which
is also explicit. The cost of the speed-up using an explicit constitutive algorithm is the
initialisation of the polynomial coefficients (30). They become rather lengthy, some mega-
bytes of source code and their derivation is only manageable by using a symbolic algebra
program.

Hill (1948) and (1979) defined a component-wise weighted norm of the stress, namely the first part of eqn (19) and the inversely weighted norm of the plastic strain increment (20). Therefore, Hill's hardening law exhibits strain-hardening and work-hardening behavior. On the other hand, the presented model simply uses the norm $\|t\| = \sqrt{t_{ij}t_{ji}}$ for the constitutive tensors which is not weighted component-wise. The hardening law, therefore, exhibits only strain-hardening behavior and no work-hardening.

The notions of normality or associated flow rules lead to confusion within the framework of the finite deformation theory, because yield functions based on different finite strain or stress definitions result in different yield surfaces, whose gradients are no longer parallel. Hence, the normality of plastic flow is strongly related to the underlying definition of finite strain or stress. Due to the transformation of the elastic strain two strain spaces are defined in the current study, namely the original $\varepsilon$-space and the transformed $\tilde{\varepsilon}$-space. We apply the normality or associated flow rule in the transformed $\tilde{\varepsilon}$-space, where we define the plastic flow by eqn (13). In general, the plastic flow rule, therefore, is non-associated to the yield function in the original $\varepsilon$-space. However, the presented model fulfils the restriction (23) of the second law of thermodynamics, as shown in Section 6. Within the framework of the infinitesimal deformation theory, the restriction (23) was formerly called Drucker's postulate (Drucker, 1952 and 1964).

The orthotropy parameters $L$, $M$, $N$, $O$, $P$, $Q$ of the presented model may be completely determined by kinematic variables, namely the plastic strain increments and the corresponding $r$-values as defined in Fig. 4, analogous to Hill's model. On the other hand, they may be determined by the static variables of the orientation-dependent yield stresses of Table 1, column two. The correlation of both sets of orthotropy parameters is a measure of the applicability of the constitutive models based on second order yield functions.

## REFERENCES

Casey, J. and Naghdi, P. M. (1983). On the nonequivalence of stress space and strain space formulations of plasticity theory. *Journal of Applied Mechanics* **50**, 350–354.

Drucker, D. C. (1952). A more fundamental approach to plastic stress–strain relations. *Proc. 1st U.S. Nat. Cong. on Applied Mechanics* [Chicago 1951], New York, pp. 487–491.

Drucker, D. C. (1964). On the postulate of stability of material in the mechanics of continua. *J. Mécanique* **3**, 235–249.

Heiduschke, K. and Sayir, M. (1989). Rotationally symmetric waves in metal rods beyond the elastic range. *Comput. Plasticity II, Proc. 2nd. Int. Conf.*, pp. 285–296 (Edited by D. R. J. Owen, E. Hinton and E. Oñate).

Heiduschke, K. (1990). Rotationssymmetrische Wellenausbreitung in Metallstäben jenseits der Elastizitätsgrenze. *Dissertation ETH* Nr 9021, Fortschr.-Ber. VDI Reihe 18, Nr 77.

Heiduschke, K., Anderheggen, E. and Reissner, J. (1991). Constitutive equations for sheet metal forming. FE-simulation of 3-D sheet metal forming processes in automotive industry, Conference with workshop, Zürich/Switzerland 14–16 May, VDI-Bericht 894, pp. 17–37.

Heiduschke, K. (1995). The logarithmic strain space description. *International Journal of Solids and Structures* **32**, 1047–1062.

Heiduschke, K. (1996). Computational aspects of the logarithmic strain space description. *International Journal of Solids and Structures* **33**, 747–760.

Hill, R. (1948). A theory of the yielding and plastic flow of anisotropic metals. *Proceedings of the Royal Society of London, Series A* **193**, pp. 281–297.

Hill, R. (1979). Theoretical plasticity of textured aggregates. *Mathematical Proceedings of the Cambridge Philosophy Society* **85**, 179–191.

Hill, R. (1987). Constitutive dual potentials in classical plasticity. *Journal of Mechanics, Physics and Solids* **35**, 23–33.

Hoesch Stahl AG, Dortmund and Krupp Stahl AG, Düsseldorf (1992). Private communications.

Krieg, R. D. and Krieg, D. B. (1977). Accuracies of numerical solution methods for the elastic-perfectly plastic model. *ASME Journal of Pressure Vessel Technology* **99**, 510–515.

Kubli, W., Anderheggen, E. and Reissner, J. (1991). Nonlinear solver with uncoupled bending and stretching deformation for simulating thin sheet metal forming. FE-simulation of 3-D sheet metal forming processes in automotive industry, Zürich/Switzerland 14–16 May, VDI-Bericht 894, pp. 325–341.

Kubli, W. (1995). Prozeßoptimierte implizite FEM-Formulierung für die Umformsimulation großflächiger Blechbauteile. *Dissertation ETH* Nr 11175.

Moss, W. C. (1984). On the computational significance of the strain space formulation of plasticity theory. *International Journal of Numerical Methods in Engineering* **20**, 1703–1709.

Naghdi, P. M. and Trapp, J. A. (1975). The significance of formulating plasticity theory with reference to loading surfaces in strain space. *International Journal of Engineering Science* **13**, 785–779.

Naghdi, P. M. and Trapp, J. A. (1975). Restrictions on constitutive equations of finitely deformed elastic–plastic materials. *Quarterly Journal of Mechanics and Applied Mathematics* **28**, 25–46.

Naghdi, P. M. (1990). A critical review of the state of finite plasticity. *Journal of Applied Mathematics and Physics* [ZAMP] **41**, 315–394.

Wolfram, S. (1991). *Mathematica*™, A system for doing mathematics by computer, 2nd edn. Addison-Wesley, Redwood City, CA.